Tetrahedron 67 (2011) 2596–2604

Contents lists available at ScienceDirect

Tetrahedron

journal homepage: www.elsevier.com/locate/tet

Synthesis and NMR spectra of the *syn* and *anti* isomers of substituted cyclobutanes—evidence for steric and spatial hyperconjugative interactions

Erich Kleinpeter *, Anica Lämmermann, Heiner Kühn

Universität Potsdam, Institut für Chemie, Karl-Liebknecht-Str. 24-25, D-14476 Potsdam (Golm), Germany

ARTICLE INFO

Article history:
Received 11 January 2011
Received in revised form 1 February 2011
Accepted 3 February 2011
Available online 4 March 2011

Keywords:
Conformational analysis
cis,cis-Tricyclo[5.3.0.0^{2,6}]dec-3-enes
NMR
DFT calculation
NBO/NCS analysis

ABSTRACT

The *syn* and *anti* isomers of *cis,cis*-tricyclo[5.3.0.0^{2,6}]dec-3-ene derivatives have been synthesized and their ^{1}H and ^{13}C NMR spectra unequivocally analyzed. Both their structures and their ^{1}H and ^{13}C NMR chemical shifts were calculated by DFT, the latter two calculations employing the GIAO perturbation method. Additionally, calculated NMR shielding values were partitioned into Lewis and non-Lewis contributions from the bonds and lone pairs involved in the molecules by accompanying NBO and NCS analyses. The differences between the *syn* and *anti* isomers were evaluated with respect to steric and spatial hyperconjugation interactions.

1. Introduction

Even if, due to the advent of multidimensional NMR spectroscopy and ultra-highfield magnets, substituent-induced ^{1}H and ^{13}C chemical shifts no longer play a significant role as structural assignment tools in NMR spectroscopy, correctly assigned ^{1}H and ^{13}C chemical shifts nevertheless still form a necessary basis for database applications, and hence remain as indispensable structural parameters. However, even for these most important NMR parameters, there is still a lack of both theoretical background and understanding of the chemical shift[1] changes due to structural variations in terms of both magnitude and direction to either higher or lower field. In this context, both Natural Bond Orbital (NBO) and Nuclear Chemical Shielding (NCS)[2] analyses can be of assistance as NBO provides information about the manner and magnitude of orbital interactions within the molecule under study whilst NCS quantitatively partitions the core, bond and lone pair electron contributions to the chemical shifts. With regards to the NMR spectra of isomers or conformers, from the differences in the chemical shifts of various ^{1}H and ^{13}C nuclei and subsequent examination in light of the orbital interactions and the partitions of orbitals with respect to their contributions to chemical shieldings, distinctions can be identified and discussed using chemist familiar models.

Herein, we employed NBO and NCS analyses[2] to evaluate the differences in the ^{1}H and ^{13}C NMR spectra of the *syn* and *anti* isomers of *cis,cis*-tricyclo[5.3.0.0^{2,6}]dec-3-ene derivatives **3a** and **4a** (Scheme 1), which were obtained via the labored hydrolysis of the tosylates of *exo*- and *endo*-7-*syn*-hydroxyl-1,2-dihydrodicyclopentadiene. Both the syntheses and detailed analyses of the ^{1}H and ^{13}C NMR spectra of **3a** and **4a** are the main objects of this manuscript.

2. Results and discussion

2.1. Chemical syntheses and NMR spectra

The attempted solvolysis of *exo*- and *endo*-7-*syn*-tosyloxy-1,2-dihydrodicyclopentadiene (**1** and **2**, respectively, Scheme 1) under usual conditions {reflux (dioxane); $NaHCO_3$} proved the extraordinary stability of these tosylates as the corresponding alcohols **1a** and **2a** were not obtained, even after 72 h. Under more drastic conditions (120 °C; sealed tube) however, hydrolysis could be enforced, though it was not **1a** and **2a** that were obtained but rather 5(*anti*)-hydroxyl-*cis,syn,cis*-tricyclo[5.3.0.0^{2,6}] dec-3-ene **3** and the corresponding *anti* isomer **4**, respectively. The alcohols were isolated in high yield as oils. Crystalline 3,5-dinitrobenzoate derivatives, **3a** and **4a**, were also prepared from **3** and **4**, respectively, by treatment of the oils with 3,5-dinitrobenzoylchloride.

The *syn*/*anti* configurations of the dicyclopentadiene derivatives **3a** and **4a** were assigned by ^{1}H[3] and ^{13}C NMR spectroscopy.[4] The detailed signal assignments of both nuclei were effected by COSY, NOESY, HSQC, and HMBC experiments. The *cis,syn,cis* stereochemistry of the

* Corresponding author. Tel.: +49 331 977 5210; fax: +49 331 977 5064; e-mail address: ekleinp@uni-potsdam.de (E. Kleinpeter).

0040-4020/$ – see front matter © 2011 Elsevier Ltd. All rights reserved.
doi:10.1016/j.tet.2011.02.012

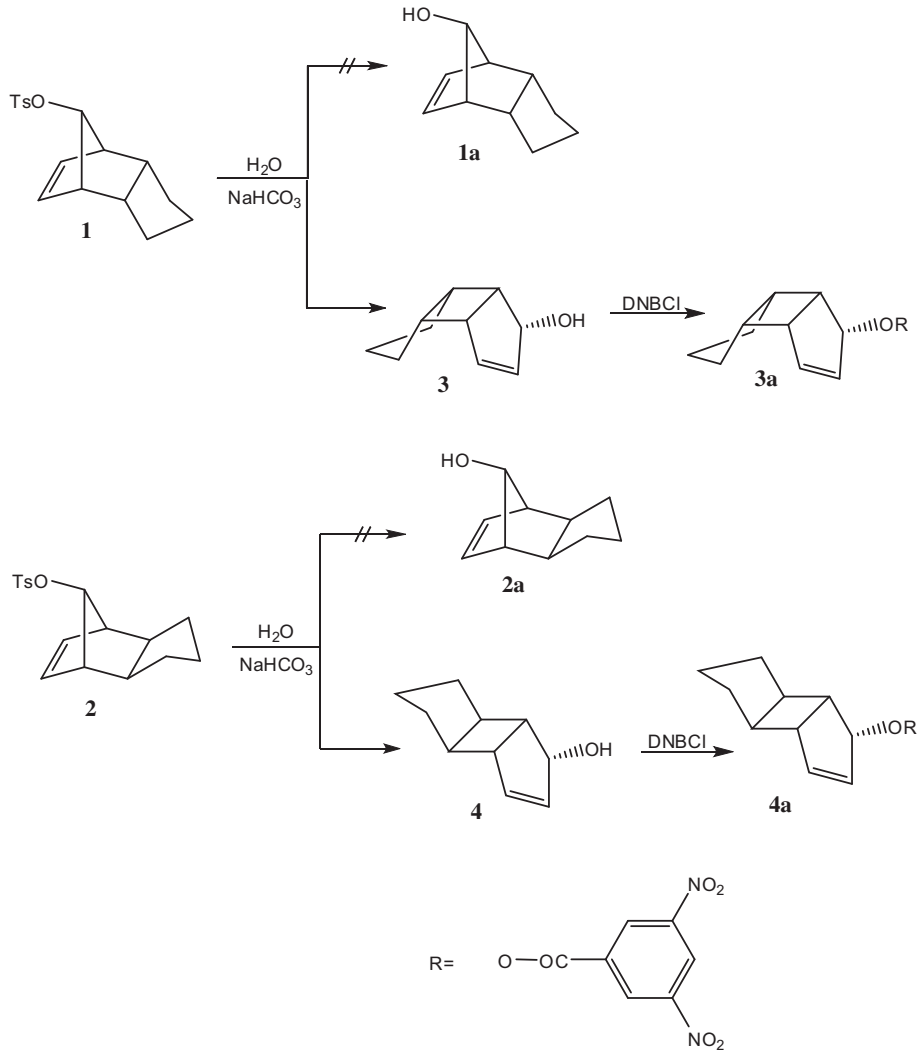

Scheme 1. The synthetic scheme for compounds **3**, **3a**, **4**, and **4a**.

two five-membered rings attached to the cyclobutane ring in **3a** was confirmed by the large vicinal coupling constants of the all-*cis*-positioned protons at the cyclobutane skeleton: $J_{11,12}$=8.5, $J_{12,16}$=6.7, $J_{11,17}$=7.5, and $J_{16,17}$=8.5 Hz. In **4a** with *cis*,*anti*,*cis* stereochemistry, these protons are partly *trans*-related and the vicinal coupling constants consequently change to: $J_{11,12}$=3.7, $J_{12,16}$=5.6, $J_{11,17}$=6.3, and $J_{16,17}$=3.7 Hz. The *anti* configuration of the hydroxyl groups in **3** and **4** (and OR groups in **3a** and **4a**, cf. Scheme 1) at C-5 in both isomers is confirmed by the relatively small $J_{15,16}$ coupling constants of ca. 2 Hz.[5] The differences in the vicinal H,H coupling constants are in agreement with results obtained for the structurally analogous bicyclo[3.2.0]heptane[6] and tricyclo[5.3.0.0^{2,6}]decane derivatives.[6–8] The experimental ^{1}H and ^{13}C NMR chemical shifts are presented in Tables 1 and 2, respectively.

The solvolytic rearrangement of the 7-substituted dicyclopentadienes is novel and establishes a new stereospecific synthetic pathway to 5-substituted *cis*,*syn*,*cis*- and *cis*,*anti*,*cis*-tricyclo[5.3.0.0^{2,6}]dec-3-enes. In the latter case, it is a useful alternative to the photochemical dimerization of cyclopentene derivatives.

2.2. Theoretical calculations

The geometries of **3a** and **4a** were fully optimized using the Gaussian03[9] program employing DFT calculations at the B3LYP/6-311+G(d,p) level of theory.[10–12] The *syn* and *anti* conformers (Scheme 2) concerning the saturated five-membered ring inversion were evaluated and, in order to describe the dynamics of this process, transition states were characterized by force constants at stationary points on the potential energy surface. The chemical shifts were calculated using the gauge-including atomic orbital (GIAO) method,[13] also at the B3LYP/6-311G(d,p) level of theory, by subtracting the shieldings of the protons in **3a** and **4a** from tetramethylsilane (TMS) used as a reference and calculated at the same

Table 1
Experimental and calculated ^{13}C NMR chemical shifts (ppm) of **3a** and **4a**

	3a expt	**3a** calculated		**4a** expt	**4a** calculated		$\Delta\delta$ of *syn*
		anti	*syn*		*anti*	*syn*	
C-1	46.71	47.35	48.28	48.69	50.84	51.16	−2.88
C-2	39.10	54.50	53.55	40.86	56.68	55.69	−2.14
C-3	141.04	152.22	149.35	143.65	152.79	152.58	−3.23
C-4	132.07	140.49	142.22	127.46	136.45	136.46	5.76
C-5	84.18	91.97	90.26	88.62	95.38	96.05	−5.79
C-6	40.75	44.56	47.42	43.86	55.18	50.39	−2.97
C-7	41.66	45.45	45.61	45.56	47.02	47.35	−1.74
C-8	28.58	33.03	31.96	32.32	39.72	37.75	−5.79
C-9	27.64	33.92	33.58	25.27	35.94	30.23	3.35
C-10	28.68	31.74	33.71	32.86	38.63	36.90	−3.19

Table 2
Experimental and calculated ^{1}H NMR chemical shifts (ppm) of **3a** and **4a**

	3a expt	**3a** calculated		**4a** expt	**4a** calculated		Δδ of *syn*
		anti	*syn*		*anti*	*syn*	
H-11	3.17	3.00	3.03	2.44	2.31	2.37	0.66
H-12	2.96	3.79	3.71	2.28	3.24	2.98	0.73
H-13	6.27	6.47	6.51	6.36	6.59	6.56	−0.05
H-14	6.15	6.53	6.50	6.00	6.39	6.40	0.10
H-15	6.03	6.01	6.26	5.82	5.93	5.95	0.31
H-16	3.62	3.10	3.18	2.89	2.71	2.44	
H-17	3.00	2.94	3.26	2.34	2.28	2.38	0.88
H-18a	1.45	1.36	1.54	1.53	1.59	1.66	−0.12
H-18e	[a]	1.80	2.00	1.74	2.25	1.78	0.22
H-19a	[a]	1.38	1.71	[b]	1.55	2.05	−0.34
H-19e	1.84	1.81	1.71	[b]	2.03	1.95	−0.24
H-20a	[a]	1.45	1.51	1.53	1.59	1.68	−0.17
H-20e	[a]	1.74	1.78	1.74	2.17	1.80	−0.02

[a] Multiplet, 1.65–1.49 ppm.
[b] Multiplet, 1.92–1.81 ppm.

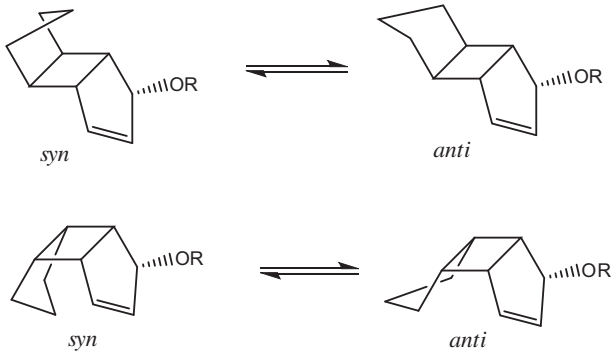

Scheme 2. Preferred conformers of the five-membered ring inversion.

level of theory. The calculated ^{1}H and ^{13}C NMR chemical shifts are also presented in Tables 1 and 2, respectively, (vide supra) with the atom numbering denoted in Scheme 3.

The experimental ^{13}C NMR chemical shifts of **3a** and **4a** were correlated with the calculated δ values of the *syn* and *anti* conformers in each case (Fig. 1). The excellent correlation obtained was strong evidence for accurately computed structures of the compounds, slightly better correlation was obtained for the *syn* conformers (cf. Scheme 2; *syn*: R^2=0.9936, *anti*: R^2=0.9905) and thus provided an initial indication that the *syn* structures are the preferred, or at least higher-populated, conformers. The corresponding correlations of the ^{1}H chemical shifts are not given because of significant signal overlap and higher order in the experimental ^{1}H NMR spectra.

2.3. Dynamic NMR spectroscopy

The ^{1}H NMR spectra of both compounds were first recorded at room temperature. The five-membered ring attached to the rigid cyclobutane skeleton should be highly flexible and, moreover, rapidly interconverting on the NMR timescale at this temperature as was indeed found to be the case. To the best of our knowledge, this dynamic ring inversion process (Scheme 2) has not been previously studied. Because extremely low barriers to ring inversion were expected,[14] the compounds were dissolved in a freon mixture (CD_2Cl_2/$CHFCl_2$/CHF_2Cl=1:1:3) and variable-temperature ^{1}H and ^{13}C NMR spectra recorded in steps down to 103 K (cf. Fig. 2 for compound **3a**). The proton signals did in fact broaden upon lowering of the temperature, with the strongest effects observed for the protons of the saturated five-membered ring. However, none of the signals were observed to decoalesce into distinct conformer signals at this bottom temperature. Examination of the corresponding *anti* isomer **4a** yielded the same result. Similar results were obtained from the low temperature ^{13}C NMR measurements of the two compounds.

Calculation of the ^{1}H chemical shift differences of the C-9 protons in **3a** and **4a** for the *syn* and *anti* conformers yielded Δν*s* of 240 and 200 Hz, respectively. Together, with a T_c<103 K and assumed values of the rate constants, k_c, of 533 and 444 s^{-1}, respectively, barriers to ring inversion of less than 4.5 kcal mol^{-1} for $\Delta G^{\neq}$ were deduced.[14] Hence, the experimentally observed broadening of the C-9 protons at 103 K corroborates the anticipated extremely low T_c of the five-membered ring inversion.

The dynamic process was also examined by DFT calculations with the theoretical treatment yielding two interesting results (cf. Table 3). Firstly, for the *cis*,*syn*,*cis* configuration of **3a**, the *syn* conformer is 0.51 kcal mol^{-1} more stable than the corresponding *anti* conformer whilst for the *cis*,*anti*,*cis* isomer **4a**, the *syn* conformer is much more stable, by 2.27 kcal mol^{-1}, than its *anti* conformer. Secondly, the calculated barrier to ring inversion was found to be very low, in the range 2.16–2.35 kcal mol^{-1}. This is in concert with the attempted experimental determination of $\Delta G^{\neq}$.

Thus, the five-membered ring inversion dynamic process remains fast on the NMR timescale even at 103 K, though evidently not that far from decoalescence. The *syn* conformer in both

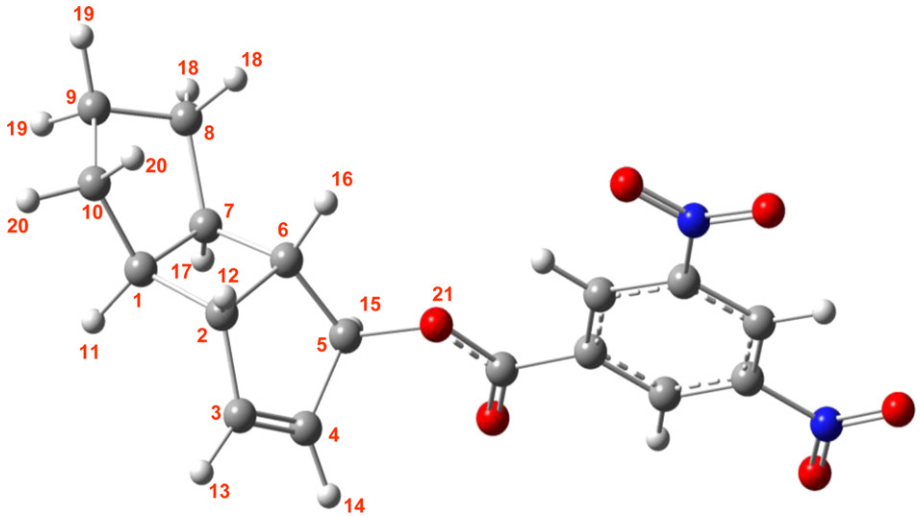

Scheme 3. Atom numbering of cyclobutane derivative **4a**.

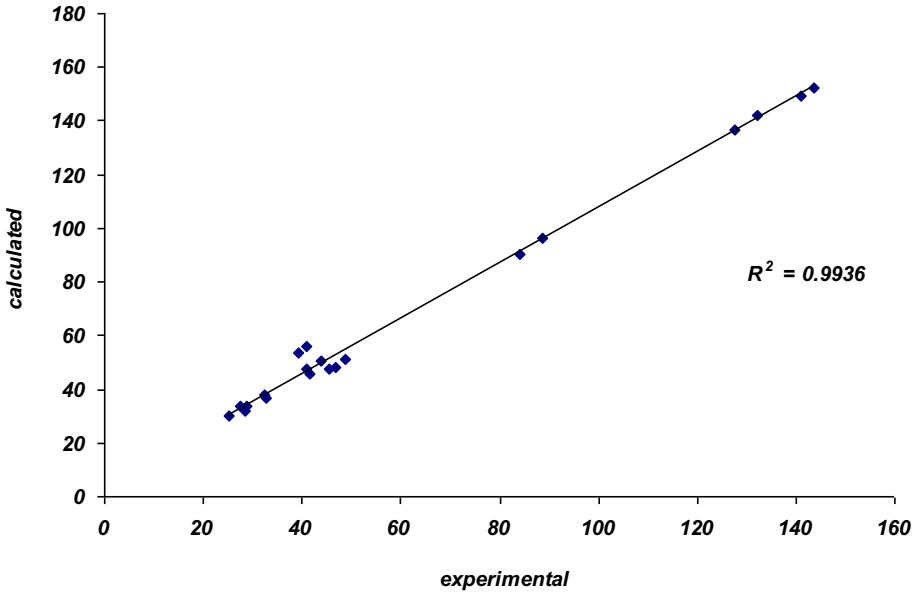

Fig. 1. Correlation of the calculated *syn* conformations δ (^{13}C) versus experimental δ (^{13}C) for *cis*,*syn*,*cis* **3a** and *cis*,*anti*,*cis* **4a**.

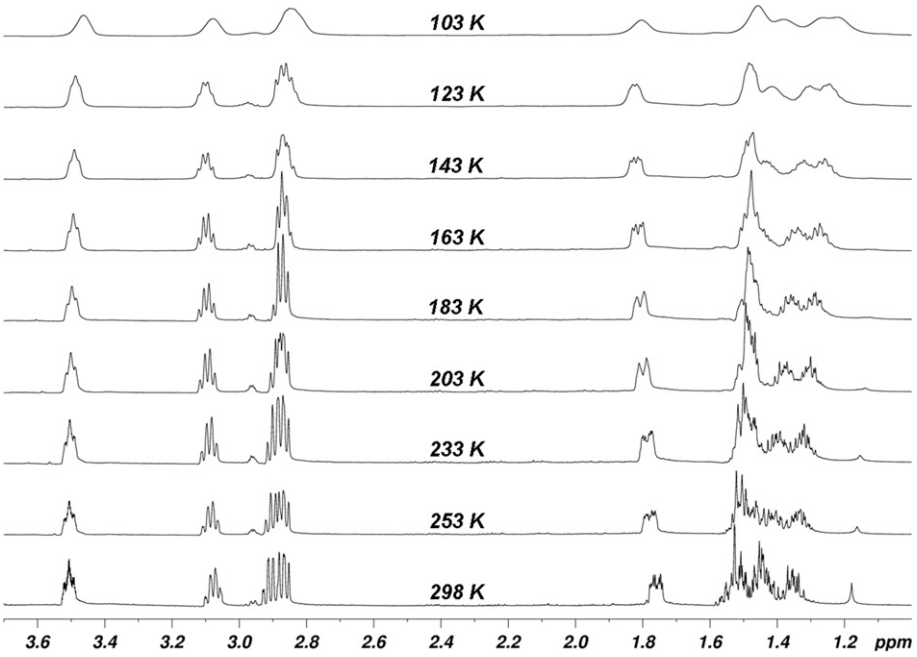

Fig. 2. Variable-temperature ^{1}H NMR spectra of the *cis*,*syn*,*cis* isomer **3a**.

Table 3
Theoretical calculation of the five-membered ring inversion barrier and preferred conformer of **3a** and **4a**

	syn (kcal mol^{-1})	*anti* (kcal mol^{-1})	Transition state (kcal mol^{-1})	Ring inversion barrier (kcal mol^{-1})
3a	0.00	0.51	2.86	2.35
4a	0.00	2.27	4.43	2.16

cis,*syn*,*cis* **3a** and *cis*,*anti*,*cis* **4a** is, surprisingly, for steric reasons, the preferred conformer. It was anticipated that the *syn* conformers should be sterically destabilized compared with the *anti* analogues and the question arises concerning the ultimate cause of this unexpected stability.

2.4. NCS analysis

Characteristic differences between the calculated chemical shifts of the *syn* conformers of *cis*,*syn*,*cis* **3a** and *cis*,*anti*,*cis* **4a** were found. For the ^{13}C chemical shifts, all carbon atoms, except for C-9 and C-4, which are deshielded, are shielded in the *cis*,*syn*,*cis* isomer with respect to the *cis*,*anti*,*cis* analogue. These stereochemical influences on ^{13}C could be due either to steric compression or to stereoelectronic effects[14] (i.e., orbital interactions of proximate bonds). A promising approach to study the effects in detail is provided by NCS analysis.[2] This method allows a partitioning of theoretical NMR GIAO[13] shieldings into magnetic contributions from core, bond, and lone pair electrons of the molecule using the NBO method.[2] In addition to computing the contributions to shieldings

from localized (or 'Lewis') bonds, this approach also computes those of a delocalized (or 'non-Lewis') nature. The NBO 5.0 program[2] was utilized by linking it directly to Gaussian 03 program.[9]

Because the behavior of C-4 and C-9 differs from the other carbon atoms and since they are in an exposed position to proximate stereochemical effects in the more stable *syn* conformer of the *cis*,*syn*,*cis* isomer **3a**, the ^{13}C chemical shifts of these two carbon atoms were studied first by NCS analysis. In Table 4, the partitions to the ^{13}C chemical shifts of both C-4 and C-9 of the *syn* conformers of *cis*,*syn*,*cis* **3a** and *cis*,*anti*,*cis* **4a** are presented together with the chemical shift differences, $\Delta\delta$, between the two isomers. A significant contribution to the deshielding of C-9 is seen to arise only from the C_9–H_{19} bond, which is *syn* positioned to the second five-membered ring moiety C-3 to C-5 ($\Delta\sigma$=−3.41 ppm; expt $\Delta\delta$=3.35 ppm). Other contributions either cancel each other out or are comparatively negligible. Contributions to C-4 are spread over a greater range of bonds but significant contributions arise from the C_3=C_4, C_4–C_5, and C_4–H_{14} bonds (altogether: $\Delta\sigma$ = −5.65 ppm; expt $\Delta\delta$=5.76 ppm) with other contributions either effectively canceling each other out or being comparatively negligible.

As has been suggested previously,[1,15] the observed ^{13}C chemical shift changes subject to stereochemical variation of a molecular structure thus arise from modifications only in the C–C and C–H bond contributions, including the carbon atom studied. Obviously in the case of C-9, only the effect of the C_9–H_{19syn} bond is influential. In the case of C-4, with the C_4–H_{14} bond less sterically congested, changes arise from the C_3–H_{13}, C_4–C_5, and C_3=C_4 bonds too. This result can only be reasonably interpreted as a steric

Table 4
NCS partitions for C-4 and C-9 in *cis*,*syn*,*cis* **3a** and *cis*,*anti*,*cis* **4a**

Bond	Lewis/non-Lewis	C-4		C-9		Δσ(C-4)	Δσ(C-9)
		cis,*syn*,*cis*	*cis*,*anti*,*cis*	*cis*,*syn*,*cis*	*cis*,*anti*,*cis*		
C_1–C_2	L	0.18	0.72	0.14	−0.08	−0.54	0.22
	NL	0.39	0.09	0.25	0.16	0.30	0.09
C_2–C_6	L	−0.35	−0.29	−0.2	−0.23	−0.06	0.03
	NL	−0.97	−0.7	−0.03	−0.05	−0.27	0.02
C_2–H_{12}	L	−1.34	−1.24	−0.07	0.15	−0.10	−0.22
	NL	1.35	1.33	0.03	−0.08	0.02	0.11
C_2–C_3	L	−9.41	−9.65	0.17	0.06	0.24	0.11
	NL	11.33	10.93	−0.13	−0.13	0.40	0.00
C_1–C_7	L	−0.07	−0.04	−1.66	−1.47	−0.03	−0.19
	NL	0.43	0.46	−0.32	−0.17	−0.03	−0.15
C_1–C_{10}	L	0.31	−0.05	−2.03	−2.32	0.36	0.29
	NL	0.12	−0.04	4.66	4.71	0.16	−0.05
C_1–H_{11}	L	−0.25	−0.26	−1.70	−1.83	0.01	0.13
	NL	0.17	0.27	1.50	1.59	−0.10	−0.09
C_6–C_7	L	−0.14	0.20	0.07	−0.09	−0.34	0.16
	NL	0.00	−0.19	−0.04	−0.02	0.19	−0.02
C_7–C_8	L	0.03	−0.15	−2.07	−2.49	0.18	0.42
	NL	0.25	0.15	1.18	1.96	0.10	−0.78
C_7–H_{17}	L	−0.13	−0.17	−0.32	−0.58	0.04	0.26
	NL	0.11	0.28	0.13	0.39	−0.17	−0.26
C_5–C_6	L	−0.44	−0.63	−0.39	0.04	0.19	−0.43
	NL	−1.25	−1.02	0.13	−0.03	−0.23	0.16
C_6–H_{16}	L	−0.02	0.07	0.06	0.19	−0.09	−0.13
	NL	0.17	0.05	0.05	−0.17	0.12	0.22
C_9–C_{10}	L	0.36	0.15	−13.82	−12.94	0.21	−0.88
	NL	0.21	0.15	−2.92	−3.76	0.06	0.84
C_{10}–H_{20a}	L	−0.24	−0.11	5.10	0.73	−0.13	4.37
	NL	0.17	0.10	−5.23	−1.65	0.07	−3.58
C_{10}–H_{20b}	L	−0.45	−0.07	0.60	5.75	−0.38	−5.15
	NL	0.29	0.11	−1.52	−5.83	0.18	4.31
C_8–C_9	L	0.31	0.05	−15.59	−15.03	0.26	−0.56
	NL	0.13	0.14	−4.13	−5.36	−0.01	1.23
C_8–H_{18a}	L	−0.19	−0.06	6.44	7.00	−0.13	−0.56
	NL	0.19	0.07	−6.98	−7.44	0.12	0.46
C_8–H_{18b}	L	−0.39	−0.19	−1.14	0.80	−0.20	−0.34
	NL	0.21	0.12	0.58	0.27	0.09	0.31
C_3–C_4	L	−66.42	−63.68	0.22	0.07	−2.74	0.15
	NL	−2.65	−2.74	−0.04	−0.03	0.09	−0.01
C_3–C_4	L	3.57	5.61	−0.44	0.03	−2.04	−0.47
	NL	0.52	−0.01	−0.30	−0.05	0.53	−0.25
C_3–H_{13}	L	−6.96	−5.78	0.11	−0.03	−1.18	0.14
	NL	2.54	1.48	−0.01	0.01	1.06	−0.02
C_4–C_5	L	−35.26	−33.38	−0.10	−0.09	−1.88	−0.01
	NL	−3.51	−3.17	−0.03	−0.03	−0.34	0.00
C_4–H_{14}	L	−47.22	−49.28	0.19	−0.04	2.06	0.23
	NL	1.63	2.53	−0.07	0.03	−0.90	−0.10
C_5–H_{15}	L	1.35	1.84	0.24	0.01	−0.49	0.23
	NL	−3.53	−4.01	−0.21	−0.01	0.48	−0.20
C_5–O_{21}	L	−1.58	−1.66	−0.15	−0.06	0.08	−0.09
	NL	0.45	0.51	0.03	0.03	−0.06	0.00
C_9–H_{19}	L	−0.24	−0.07	−27.43	−26.95	−0.17	−0.48
	NL	0.17	0.06	6.25	6.00	0.11	0.25
C_9–H_{19}	L	−1.07	−0.28	12.26	15.67	−0.79	−3.41
	NL	0.37	0.17	−3.91	−4.24	0.20	0.33

interaction between H-19*syn* and the C_5–$C_4(H_{14})$=C_3 moiety in the *cis*,*syn*,*cis* isomer **3a** (compared with the *cis*,*anti*,*cis* isomer **4a**), even if the effect is deshielding (steric compression on ^{13}C is signified by shielding resulting from steric *γ-gauche* interactions[14]). However, this is not a contradiction because the *δ*-effect is a deshielding one though the steric hindrance is ever larger than in comparable *γ-gauche* fragments.[1,14,15]

Concerning the ^{13}C chemical shifts of the remaining carbon atoms, which are shielded with respect of *cis*,*anti*,*cis* **4a** in comparison to *cis*,*syn*,*cis* **3a**, partitions to the ^{13}C chemical shifts of C-3, C-2, C-1, and C-10 and shielding differences are given in Table 5. From this analysis, the following results were obtained:

	Proximate bonds	More distant bonds	Δσ (Δδ)/ppm
C-3	C_3=C_4, C_3–H_{13}, C_2–C_3 (3.52)	C_1–C_2, C_1–C_7, C_1–C_{10}, C_1–H_{11} (0.45)	3.97 (−3.23)
C-2	C_2–C_6, C_1–C_2, C_2–C_3, C_2–H_{12} (2.10)	C_{10}–C_{20}, C_1–H_{11}, C_{10}–H_{20anti} (0.35)	2.45 (−2.14)
C-1	C_1–C_2, C_2–C_3, C_1–C_7, C_1–C_{10}, C_1–H_{11} (1.31)	C_2–C_6, C_2–H_{12}, C_9–C_{10}, C_{10}–$H_{20syn,anti}$ C_9–$H_{19syn,anti}$ (0.87)	2.18 (−2.88)
C-10	C_1–C_7, C_1–C_{10}, C_9–C_{10}, C_{10}–H_{20syn}, C_{10}–H_{20anti} (2.49)	C_1–C_2, C_2–H_{12} (1.27)	3.76 (3.19)

Again, differences in C–C and C–H bond contributions, including the carbon atom studied, form the main basis for distinction.[1] In the case of these ^{13}C chemical shifts however, more distant bond partitions also contribute. This is readily comprehensible: during the inversion of the *anti* isomer **4a** to the *syn* isomer **3a**, not only proximate bonds, but also more distant bond partitions change because the whole stereochemistry of the skeleton is altered completely. This is actually well proven by the corresponding shielding variations given in the aforementioned shielding partitioning survey. Identical conclusions can be drawn if the corresponding effects on the ^{13}C chemical shifts of the remaining carbon atoms are examined. The ^{13}C chemical shift differences between *cis*,*anti*,*cis* **4a** and *cis*,*syn*,*cis* **3a** should relate to the differences in steric hindrance experienced by the isomers and the bonds of the molecules, which are involved. This in fact can be readily identified by NCS analysis. If orbital interactions are involved too, these will become apparent from the ensuing NBO analysis.

The corresponding proton shifts of the isomers are also influenced by the change of stereochemistry, though they differ in size and direction. While the ^1H nuclei of the five-membered rings are only modestly influenced ($\Delta\delta$ <0.3 ppm), much stronger shielding variations are observed for the four-membered ring protons H-11 to H-12 and H-17 ($\Delta\delta$ up to 0.88 ppm). In the more congested *cis*,*syn*,*cis* **3a** isomer, the ^1H chemical shifts are all deshielded, in excellent agreement with the corresponding ^{13}C chemical shifts, which are all shielded (vide supra). In terms of steric compression, this means reduced steric congestion[14] for the corresponding four-membered ring C–H bonds in the *cis*,*syn*,*cis* **3a** isomer as suggested. The corresponding NCS analysis of the ^1H chemical shieldings of **3a** and **4a** is given in the ESI.

Structural evidence for the presence of considerable steric strain in the *syn* conformation of the *cis*,*syn*,*cis* isomer **3a** extends to distortions that are apparent in the $\sigma(C_9$–$H_{19syn})$, $\sigma(C_{10}$–$H_{20syn})$, and $\pi(C_3$=$C_4)$ orbitals of this structure and which are depicted in Fig. 3. These structural perturbations clearly indicate the presence of steric strain, which undoubtedly must have an influence on the ^{13}C and ^1H chemical shifts involved and must be accounted for. Distortions of the π cloud have been reported previously by Martin et al.[16,17] along with short distances of one methane proton above the π system in supramolecules, supporting the suggestion of van der Waals orbital compression effects to be the cause of shielding/deshielding changes.

Table 5
Differences (Δσ) of NCS partitions for C-3, C-2, C-10, and C-1 for the *syn* conformations of *cis*,*syn*,*cis* **3a** and *cis*,*anti*,*cis* **4a**

Bond	Lewis/non-Lewis	Δσ(C-2)[a]	Δσ(C-1)[a]	Δσ(C-10)[a]	Δσ(C-3)[a]
C_1–C_2	L	1.62	1.84	0.64	−1.7
	NL	0.34	0.15	0.03	1.06
C_2–C_6	L	−0.22	0.47	−0.14	−0.32
	NL	0.53	−0.23	−0.05	0.54
C_2–H_{12}	L	0.28	0.50	0.13	1.25
	NL	0.51	−0.04	0.47	−1.13
C_2–C_3	L	−2.02	−1.11	0.20	0.00
	NL	1.15	0.76	−0.19	1.02
C_1–C_7	L	0.31	2.18	−0.32	0.00
	NL	−0.41	−1.27	0.87	−0.53
C_1–C_{10}	L	−1.27	0.00	2.47	−1.01
	NL	1.85	1.12	−1.96	1.63
C_1–H_{11}	L	−0.26	−5.02	0.90	1.28
	NL	−0.89	2.66	−0.82	−0.28
C_6–C_7	L	0.45	−0.17	0.09	−0.27
	NL	−0.44	−0.01	−0.13	0.08
C_7–C_8	L	−0.10	−1.11	−0.13	0.07
	NL	−0.06	0.82	0.01	0.08
C_7–H_{17}	L	0.03	1.61	0.04	0.04
	NL	0.02	−1.62	0.07	0.00
C_5–C_6	L	−0.35	−0.07	−0.17	−0.02
	NL	0.10	0.01	0.01	0.04
C_6–H_{16}	L	0.20	0.10	−0.08	0.05
	NL	−0.30	0.00	0.16	0.01
C_9–C_{10}	L	−0.01	0.00	−0.46	0.24
	NL	−0.11	−0.32	−1.66	0.01
C_{10}–H_{20a}	L	0.87	5.67	−21.57	−0.19
	NL	0.05	−4.36	8.70	0.26
C_{10}–H_{20b}	L	0.16	−4.71	24.89	−0.92
	NL	−0.02	3.42	−8.42	0.80
C_8–C_9	L	−0.13	0.03	−0.13	0.14
	NL	0.03	0.08	−0.14	0.07
C_8–H_{18a}	L	0.04	0.15	0.22	−0.09
	NL	−0.09	−0.12	−0.12	0.12
C_8–H_{18b}	L	−0.02	−0.17	0.18	−0.09
	NL	−0.12	0.23	−0.09	0.03
C_3–C_4	L	−0.37	−0.06	0.14	1.27
	NL	0.15	0.00	0.01	−0.05
C_3–C_4	L	0.23	0.33	−0.91	0.15
	NL	−0.25	0.67	0.19	0.03
C_3–H_{13}	L	0.78	−0.11	0.05	−0.68
	NL	−0.77	0.08	0.10	1.23
C_4–C_5	L	−0.08	−0.09	−0.05	0.05
	NL	0.15	0.01	0.00	−0.68
C_4–H_{14}	L	−0.05	−0.06	0.14	−0.37
	NL	0.13	0.02	−0.05	0.40
C_5–H_{15}	L	0.07	−0.02	0.09	−0.05
	NL	0.03	0.00	−0.09	0.08
C_5–O_{21}	L	−0.07	−0.03	−0.06	−0.12
	NL	−0.02	0.01	0.00	0.02
C_9–H_{19}	L	−0.05	0.31	−0.24	−0.14
	NL	0.05	−0.09	0.29	0.21
C_9–H_{19}	L	0.20	0.32	0.62	−0.48
	NL	−0.15	−0.07	−0.64	0.21

[a] Δσ=*cis*,*syn*,*cis* **3a**–*cis*,*anti*,*cis* **4a**.

2.5. NBO analysis

In the *cis*,*syn*,*cis* isomer **3a**, some stereoelectronic interactions between the two five-membered ring moieties could be detected as the main result of the NBO study; the corresponding orbital interaction energies are given in Fig. 4.

A hydrogen bonding-like donation of the C_{10}–H_{20syn} orbital into the antibonding π-orbital of the C_3=C_4 double bond $[\sigma(C_{10}$–$H_{20syn}) \rightarrow \pi^*(C_3$=$C_4)]$ is present in the *anti* conformer. This interaction amounts to 0.54 kcal mol^{-1} (the distance between H-20*syn* and the C_3=C_4 double bond is 3.33 Å) and adequately

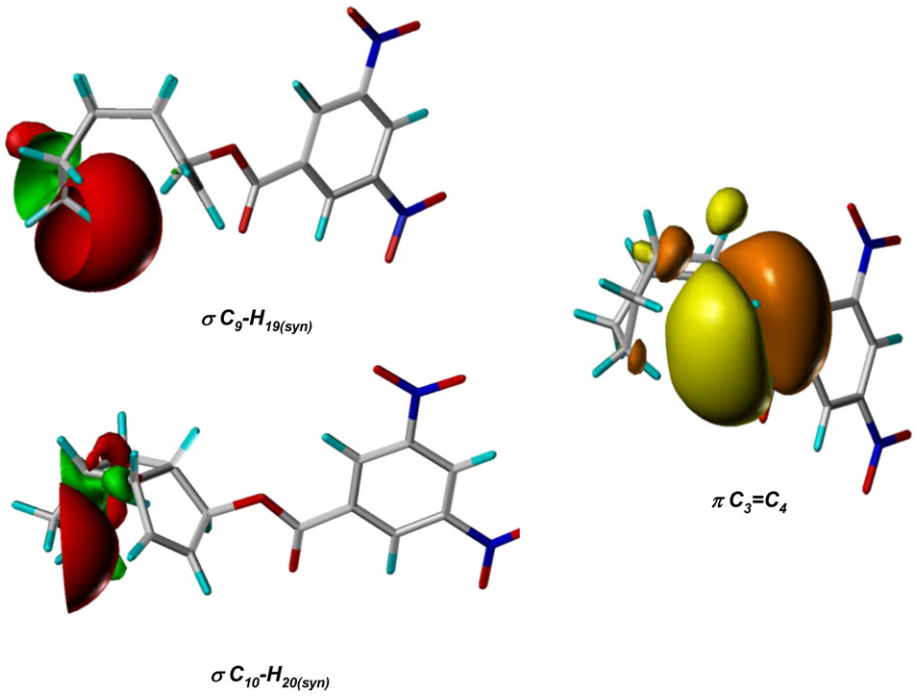

Fig. 3. The $\sigma(C_9{-}H_{19syn})$, $\sigma(C_{10}{-}H_{20syn})$, and $\pi(C_3{=}C_4)$ orbitals of the *cis*,*syn*,*cis* isomer **3a**. The distortions of these orbitals due to steric interactions with each other are clearly evident.

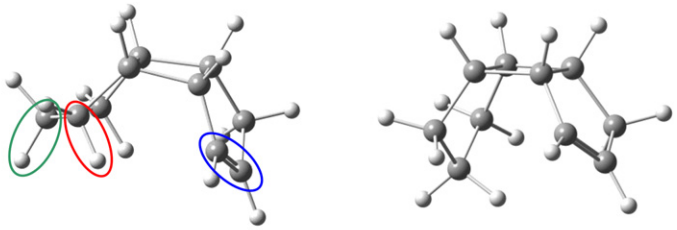

distances:		
C_{10}-H_{20} → C_3=C_4	3.25 Å	3.33 Å
C_9H_{19} → C_3=C_4	4.44 Å	3.18 Å

Hyperconjugative interactions:		
σ C_{10}-H_{20} → π* C_3=C_4	0.54	0.26 kcal/mol
σ C_9H_{19} → π* C_3=C_4	0.00	0.08 kcal/mol
π C_3=C_4 → σ* C_{10}-H_{20}	0.13	0.00 kcal/mol
π C_3=C_4 → σ* C_9H_{19}	0.00	0.26 kcal/mol

Fig. 4. Orbital interaction energies in the *syn* and *anti* conformers of *cis*,*syn*,*cis* **3a**.

stabilizes the *cis*,*syn*,*cis* isomer **3a** because in the *cis*,*anti*,*cis* isomer **4a**, these kind of interactions were neither obtained nor expected. Back donation, $\pi(C_3{=}C_4){\rightarrow}\sigma^*(C_{10}{-}H_{20syn})$, is observed in **3a** as well; however it is energetically quite small and only amounts to 0.13 kcal mol^{-1}. The same interactions are observed for H-20*anti*, but are of much lower magnitude. In the corresponding *syn* conformer, there is still some influence from these interactions, though it is of smaller magnitude. By contrast, the corresponding $\sigma(C_9{-}H_{19syn}){\rightarrow}\pi^*(C_3{=}C_4)$ remains small to negligible in both conformers and only in the *syn* conformer does back donation by $C_{19}{-}H_{19syn}$ increase. This is quite surprising because the distance from H-19*syn* to the $C_3{=}C_4$ double bond is much shorter in the *syn* conformer of *cis*,*syn*,*cis* **3a** where it is only 3.18 Å.

In summary, for *cis*,*syn*,*cis* **3a**, spatial orbital interactions between the two five-membered ring moieties stabilize this isomer in both the *syn* and *anti* conformations. Hyperconjugative orbital interactions between $C_{10}{-}H_{20syn}$ and $C_9{-}H_{19syn}$ on the one side with the $C_3{=}C_4$ double bond on the other, unsaturated side of **3a** are responsible for this. To clarify the influence of spatial proximity on the structure of **3a**, NBO calculations of several related molecules were performed with the following main results depicted in Fig. 5 and detailed below:

(i) 3,5-Dinitrobenzoyl substitution in position 1 is of no influence and the same orbital interaction stabilizing energies were observed. For this reason, in subsequent calculations the 1-substituent was omitted.

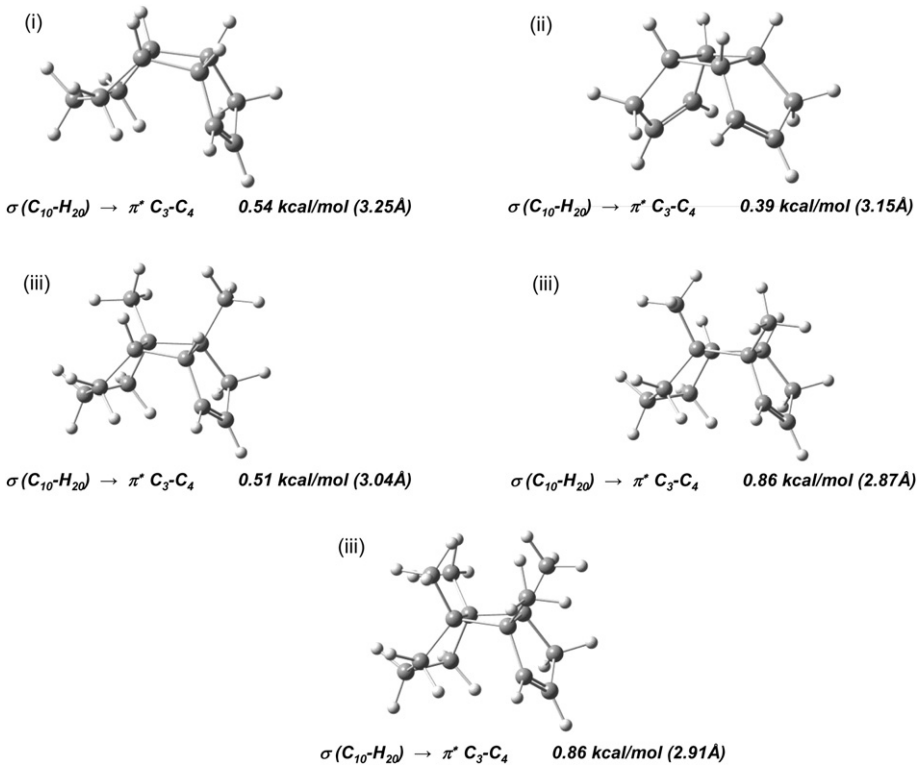

Fig. 5. Orbital interaction energies in the *syn* and *anti* conformers of *cis*,*syn*,*cis* **3a** and related dimethyl and tetramethyl derivatives.

(ii) The $\sigma(C_{10}{-}H_{20syn}) \rightarrow \pi^*(C_3{=}C_4)$ orbital interaction is reduced if the second five-membered ring moiety is partially unsaturated too. Only a value of 0.39 kcal mol^{-1} was calculated in line with a flow of electron density into the inner ring $C_8{=}C_9$ double bond.

(iii) Dimethyl substitution of the four-membered ring moiety at C-6 and C-7 is of no influence but at C-1 and C-2, it is of major influence. Both bonds are more proximate (2.87 Å) and the orbital stabilization energy increases to 0.86 kcal mol^{-1}. Tetramethyl substitution has a similar effect (2.91 Å and 0.86 kcal mol^{-1}).

As expected, the orbital interaction energy is distant dependent with a greater effect observed with closer proximity. Thus, consequently, the more congested the molecule, thereby leading to steric destabilization, the more effective the present spatial orbital interactions are. Hence, a net balance between the two competing effects thus determines both the structure and stability of the resulting *syn* or *anti* conformers in the *cis*,*syn*,*cis* **3a** and *cis*,*anti*,*cis* **4a** isomers.

3. Conclusions

The *syn* and *anti* isomeric derivatives, **3a** and **4a**, respectively, of *cis*,*cis*-tricyclo[5.3.0.$0^{2,6}$]dec-3-ene have been synthesized and their ^1H and ^{13}C NMR spectra recorded and unequivocally assigned. The synthesis of these compounds opens up a new stereospecific path from the corresponding 7-substituted dicyclopentadiene derivatives as a useful alternative to the photochemical dimerization of cyclopentenes.

The dynamic process of the five-membered ring inversion is fast on the NMR timescale even at 103 K ($\Delta G^{\neq}$ <4.5 kcal mol^{-1}); this experimental observation is corroborated by theoretical calculations. From the theoretical calculations and by correlations of $\Delta\delta$ ($^{13}C_{calcd}$) versus $\Delta\delta$ ($^{13}C_{expt}$), the *syn* conformers were identified as the preferred conformers in both **3a** and **4a**. Because this result was very surprising in the case of *cis*,*syn*,*cis* **3a**, detailed NBO and NCS analyses were performed. It was found that the two five-membered ring moieties in the *syn* conformer of *cis*,*syn*,*cis* **3a** experience not only strong steric hindrance, but also stabilizing, distance dependent orbital interactions, e.g., $\pi(C_3{=}C_4) \rightarrow \sigma^*(C_{10}{-}H_{20syn})$. Thus, contrastingly, the more congested the isomer (resulting in greater steric destabilization), the more effective the stabilizing spatial orbital interactions are. Hence, a net balance between the two competing effects determines both the structure and stability of the *syn*/*anti* conformers in the *cis*,*syn*,*cis* **3a** and *cis*,*anti*,*cis* **4a** isomers. Accordingly, the *syn* conformer of *cis*,*anti*,*cis* **4a** is practically anancomeric.

4. Experimental

4.1. General

All melting points were determined on a Boetius micro hotstage microscope (Fa. Analytik Dresden). IR spectra (KBr) were recorded with a Perkin–Elmer FT-IR 1600 spectrometer. The mass spectra were recorded with a Finnigan-MAT SSQ 710 (70 eV). ESI-MS spectra were obtained in positive ion mode using a Q-TOF_{micro} mass spectrometer (Micromass Manchester, UK) equipped with an ESI source; analyte solutions were injected using a syringe pump (Harvard Apparatus Ltd., Edenbridge, UK) at flow rates ranging from 2 to 20 μL/min whilst the capillary voltage was set to 2.6 kV. Elemental compositions were determined by accurate measurements with deviations less than 10 ppm from the calculated values. Elemental analyses were performed on an autoanalyzer CHNS-932 (Fa. Leco Instruments GmbH) with acceptable compositions for all compounds (viz. C, H, and N all within ±3% of calculated values). ^1H and ^{13}C NMR spectra were recorded on Bruker Avance 500 or 300 MHz spectrometers using 5 mm probes operating at 500 and

300 MHz for ^{1}H, respectively, and 125 and 75 MHz for ^{13}C, respectively, whilst low temperature NMR spectra were recorded on a Bruker Avance 600 (operating at 600 and 150 MHz for ^{1}H and ^{13}C, respectively). Chemical shifts were determined internally relative to residual $CHCl_3$ (^{1}H, δ 7.27 ppm), $CDCl_3$ (^{13}C, δ 77.0 ppm) or CD_2Cl_2 (^{13}C, δ 53.73 ppm) and are given in parts per million downfield from TMS (=0 ppm for both ^{1}H and ^{13}C). Analysis and assignment of the ^{1}H NMR data were supported by homonuclear (COSY and NOESY) and heteronuclear ($^{1}H\{^{13}C\}$-HSQC and $^{1}H\{^{13}C\}$-HMBC) 2D correlation experiments. A solvent mixture of CD_2Cl_2, $CHFCl_2$, and CHF_2Cl in a ratio of 1:1:3 was used for the low-temperature measurements. The probe temperature was calibrated by means of a PT 100 thermocouple inserted into a dummy tube.

4.2. General procedure for the synthesis of 5(*anti*)–hydroxyltricyclo[5.3.0.0^{2,6}]dec-3-ene derivatives

Separate compounds of (*exo*/*endo*)-7(*syn*)-tosyloxy-1,2-dihydrodicyclopentadiene (2 g, 6.6 mmol) together with water (10 mL), dioxane (30 mL), and $NaHCO_3$ (2 g, 24 mmol) were heated for 24 h at 130 °C in an autoclave. After cooling, water was added to the reaction and the mixture extracted with portions of ether. The ether fractions were combined, washed with water, and then dried over Na_2SO_4. After filtration, the solution was concentrated under reduced pressure to yield a yellow oil, which was purified by column chromatography (Al_2O_3 neutral, activity I, *n*-pentane/diethylether 3:1).

*4.2.1. 5(anti)-Hydroxy-cis,syn,cis-tricyclo[5.3.0.0^{2,6}]dec-3-ene (**3**).* Compound **3** was synthesized from 7(*syn*)-tosyloxy-1,2-dihydro-*endo*-dicyclopentadiene following the general procedure in 73% yield as a colorless oil. Anal. Calcd for $C_{10}H_{14}O$: C, 79.95; H, 9.39; found: C, 80.56; H, 8.79; ^{1}H NMR (ppm, $CDCl_3$): 5.93 (m, 2H, CH=CH), 4.68 (m, 1H, C*H*OH), 3.40 (m, 1H, H-12), 2.60 (m, 1H, H-16), 2.90 (m, 2H, H-11, H-17); $J_{13,14}$=5.5, $J_{15,16}$=1, $J_{11,12}$=8.5, $J_{12,16}$=6.7, $J_{11,17}$=7.5, and $J_{16,17}$=8.5 Hz.

*4.2.2. 5(anti)-(3,5-Dinitrobenzoyloxy)-cis,syn,cis-tricyclo[5.3.0.0^{2,6}]dec-3-ene (**3a**).* Compound **3a** was obtained from **3** by treatment with 3,5-dinitrobenzoylchloride in pyridine to yield slightly yellow needles, mp 102–103 °C. Anal. Calcd for $C_{17}H_{16}N_2O_6$: C, 59.30; H, 4.68; N, 8.14; found: C, 58.24; H, 4.65; N, 7.19; IR (cm^{-1}, KBr): 1165, 1273 (C–O), 1550, 1625 (C=C, aromatic), 1720 (C=O), 3070 (C–H, alkene), 3095, 3115 (C–H, aromatic); ^{1}H NMR (ppm, $CDCl_3$): 9.08 (m, 3H, aromatic), 6.27 and 6.15 (m, 2H, CH=CH), 6.03 (m, 1H, C*H*–ODNB).

*4.2.3. 5(anti)-Hydroxy-cis,anti,cis-tricyclo[5.3.0.0^{2,6}]dec-3-ene (**4**).* Compound **4** was synthesized from 7(*syn*)-tosyloxy-1,2-dihydro-*exo*-dicyclopentadiene following the general procedure in 76% yield as colorless oil. Anal. Calcd for $C_{10}H_{14}O$: C, 79.95; H, 9.39; found: C, 78.15; H, 9.02; ^{1}H NMR (ppm, $CDCl_3$): 5.99 (m, 1H, CH=CH), 5.78 (m, 1H, CH=CH), 4.46 (t, 1H, C*H*OH), 2.65 (m, 1H, H-12), 2.14 (m, 1H, H-16); $J_{13,14}$=5.4, $J_{15,16}$=1, $J_{11,12}$=$J_{16,17}$=3.7, $J_{12,16}$=5.6, $J_{11,17}$=6.3, and $J_{12,13}$=2.4 Hz.

*4.2.4. 5(anti)-(3,5-Dinitrobenzoyloxy)-cis,anti,cis-tricyclo[5.3.0.0] dec-3-ene (**4a**).* Compound **4a** was obtained from **4** by treatment with 3,5-dinitrobenzoylchloride in pyridine to yield slightly yellow needles, mp 144 °C. Anal. Calcd for $C_{17}H_{16}N_2O_6$: C, 59.30; H, 4.68; N, 8.14; found: C, 60.84; H, 5.28; N, 7.43; IR (cm^{-1}, KBr): 1169, 1271 (C–O), 1550, 1627 (C=C, aromatic), 1720 (C=O), 3060–3103 (C–H, alkene, aromatic); ^{1}H NMR (ppm, $CDCl_3$): 9.09 (m, 3H, aromatic), 6.59 and 6.39 (m, 2H, CH=CH), 5.93 (m, 1H, C*H*–ODNB), 3.24 (m, 1H, H-12); $J_{13,14}$=5.4 and $J_{12,13}$=2.8 Hz; MS *m*/*e* (ion, relative intensity): 345 ($[M+1]^+$, 2), 276 ($C_{12}H_8N_2O_6^+$, 14), 195 ($C_7H_3N_2O_5^+$, 91).

Acknowledgements

Dr. Karel D. Klika is thanked for language correction of the manuscript.

Supplementary data

Supplementary data associated with this article contain atomic coordinates, NBO/NCS data, and $^{1}H/^{13}C$ NMR spectra of **3a**/**4a**(*syn*/*anti*). Supplementary data associated with this article can be found in online version at doi:10.1016/j.tet.2011.02.012.

References and notes

1. Kleinpeter, E.; Seidl, P. R. *J. Phys. Org. Chem.* **2004**, *17*, 680.
2. (a) Bohmann, J. A.; Weinhold, F.; Farrar, T. C. *J. Chem. Phys.* **1997**, *107*, 1173; (b) NBO 5.0: Glendenig, E. D.; Badenhoop, J. K.; Reed, A. E.; Carpenter, J. E.; Bohmann, J. A.; Morales, C. M.; Weinhold, F. *Theoretical Chemistry*; Institute, University of Wisconsin: Madison, 2001; and updates.
3. Kleinpeter, E.; Kühn, H.; Mühlstädt, M. *Org. Magn. Reson.* **1976**, *8*, 261.
4. (a) Kleinpeter, E.; Kühn, H.; Mühlstädt, M. *Org. Magn. Reson.* **1976**, *8*, 279; (b) Kleinpeter, E.; Kühn, H.; Mühlstädt, M.; Jancke, H.; Zeigan, D. *J. Prakt. Chem.* **1982**, *324*, 609; (c) Kleinpeter, E.; Kühn, H.; Mühlstädt, M.; Pihlaja, K. *Finn. Chem. Lett.* **1982**, 25.
5. Bongini, A.; Lamartina, L.; Mondelli, R.; Tagliabue, G. *Org. Magn. Reson.* **1975**, *7*, 320.
6. Klinsmann, U.; Gauthier, J.; Schaffner, K.; Pasternak, M.; Fuchs, B. *Helv. Chim. Acta* **1972**, *55*, 266.
7. Eaton, P. E.; Cerefice, S. A. *J. Chem. Soc., Chem. Commun.* **1970**, 1494.
8. Breslow, R.; Hoffman, J. M., Jr. *J. Am. Chem. Soc.* **1972**, *94*, 2111.
9. Frisch, M. J.; Trucks, G. W.; Schlegel, H. B.; Scuseria, G. E.; Robb, M. A.; Cheeseman, J. R.; Montgomery, J. A., Jr.; Vreven, T.; Kudin, K. N.; Burant, J. C.; Millam, J. M.; Iyengar, S. S.; Tomasi, J.; Barone, V.; Mennucci, B.; Cossi, M.; Scalmani, G.; Rega, N.; Petersson, G. A.; Nakatsuji, H.; Hada, B.; Ehara, M.; Toyota, K.; Fukuda, R.; Hasegawa, J.; Ishida, M.; Nakajima, T.; Honda, Y.; Kitao, O.; Nakai, H.; Klene, M.; Li, X.; Knox, J. E.; Hratchian, H. P.; Cross, J. B.; Adamo, C.; Jaramillo, J.; Gomperts, R.; Stratmann, R. E.; Yazyev, O.; Austin, A. J.; Cammi, R.; Pomelli, C.; Ochterski, J. W.; Ayala, P. Y.; Morokuma, K.; Voth, G. A.; Salvador, P.; Dannenberg, J. J.; Zakrzewski, V. G.; Dapprich, S.; Daniels, A. D.; Strain, M. C.; Farkas, O.; Malick, D. K.; Rabuck, A. D.; Raghavachari, K.; Foresman, J. B.; Ortiz, J. V.; Cui, Q.; Baboul, A. G.; Clifford, S.; Cioslowski, J.; Stefanov, B. B.; Liu, G.; Liashenko, A.; Piskorz, P.; Komaromi, I.; Martin, R. L.; Fox, D. J.; Keith, T.; Al-Laham, M. A.; Peng, C. Y.; Nanayakkara, A.; Challacombe, M.; Gill, P. M. W.; Johnson, B.; Chen, W.; Wong, M. W.; Gonzalez, C.; Pople, J. A. *Gaussian 03, revision C.02*; Gaussian, Inc.: Pittsburgh, PA, 2004.
10. Becke, A. D. *J. Chem. Phys.* **1993**, *98*, 5648.
11. Lee, C.; Yang, W.; Parr, R. G. *Phys. Rev. B* **1988**, *37*, 785.
12. Ditchfield, R.; Hehre, W. J.; Pople, J. A. *J. Chem. Phys.* **1971**, *54*, 724.
13. Ditchfield, R. *Mol. Phys.* **1974**, *27*, 789.
14. Pihlaja, K.; Kleinpeter, E. Carbon-13 NMR Chemical Shifts in Structural and Stereochemical Analysis In *Methods in Stereochemical Analysis*; Marchand, A. P., Ed.; VCH: New York, NY, 1994.
15. Kleinpeter, E.; Klod, S. *J. Am. Chem. Soc.* **2004**, *126*, 2231.
16. Martin, J. N. H.; Facelli, C.; de Dios, A. C. Modeling NMR Chemical Shifts: Gaining Insights into Structure and Environment In. *ACS Symposium Series*; American Chemical Society: Washington, DC, 1999; Vol. 732, pp 207–219.
17. Martin, N. H.; Nance, K. H. *J. Mol. Graph. Model.* **2002**, *21*, 51.